Hughes, D. C., Turner, D. C., Baehr, L. M., Seaborne, R. A., Viggars, M., Jarvis, J. C., Gorski, P. P., Stewart, C. E., Owens, D. J., Bodine, S. C., Sharples, A. (2020). Knockdown of the E3 Ubiquitin ligase UBR5 and its role in skeletal muscle anabolism. *American Journal of Physiology - Cell Physiology, 320*(1), C45-C56. http://dx.doi.org/10.1152/ajpcell.00432.2020

Knockdown of the E3 Ubiquitin ligase UBR5 and its role in skeletal muscle anabolism

David C. Hughes*[4], Daniel C. Turner[1,2,3]*, Leslie M. Baehr[4]*, Robert A. Seaborne[3,5], Mark Viggars[3], Jonathan C. Jarvis[3], Piotr P. Gorski[1,2], Claire E. Stewart[3], Daniel J. Owens[3], Sue C. Bodine[4#] and Adam P. Sharples[1,2,3#]

[1]*Institute for Physical Performance, Norwegian School of Sport Sciences (NiH), Oslo, Norway*

[2]*Inst. for Science & Technology in Medicine (ISTM), School of Pharmacy and Bioengineering, Keele University, Staffordshire, UK*

[3]*Stem Cells, Ageing and Molecular Physiology Unit (SCAMP), Research Institute for Sport & Exercise Sciences (RISES), Liverpool John Moores University, Liverpool, UK*

[4]*Department of Internal Medicine, Division of Endocrinology and Metabolism, Carver College of Medicine, University of Iowa, Iowa City, IA, USA*

[5]*Centre for Genomics and Child Health, Blizard Institute, Barts and the London School of Medicine and Dentistry, Queen Mary University of London, UK*

* Primary Authors. These authors contributed equally to this work.

Corresponding authors

Corresponding Authors Details:

Sue C. Bodine & Adam P. Sharples

Email: sue-bodine@uiowa.edu & a.p.sharples@googlemail.com

Abstract

UBR5 is an E3-ubiquitin-ligase positively associated with anabolism, hypertrophy and recovery from atrophy in skeletal muscle. The precise mechanisms underpinning UBR5's role in the regulation of skeletal muscle mass remains unknown. The present study aimed to elucidate these mechanisms by silencing the UBR5 gene *in-vivo*. To achieve this aim, we electroporated a UBR5-RNAi plasmid into mouse tibialis anterior muscle to investigate the impact of reduced UBR5 on mechano-transduction signalling MEK/ERK/p90RSK and Akt/GSK3β/p70S6K/4E-BP1/rpS6 pathways. Seven days post UBR5 RNAi electroporation, while reductions in overall muscle mass were not detected, mean CSA of GFP-positive fibers was reduced (-9.5%) and the number of large fibers was lower versus the control. Importantly, UBR5-RNAi significantly reduced total RNA, muscle protein synthesis, ERK1/2, Akt and GSK3β activity. Whilst p90RSK phosphorylation significantly increased, total p90RSK protein levels demonstrated a 45% reduction with UBR5-RNAi. Finally, these early events after 7 days of UBR5 knockdown culminated in significant reductions in muscle mass (-4.6%) and larger reductions in fiber CSA (-18.5%) after 30 days. This was associated with increased levels of the phosphatase PP2Ac, and inappropriate chronic elevation of p70S6K and rpS6 between 7 and 30 days, and corresponding reductions in eIF4e. This study demonstrates UBR5 plays an important role in anabolism/hypertrophy, whereby knockdown of UBR5 culminates in skeletal muscle atrophy.

Running title: UBR5 knockdown and skeletal muscle anabolism

Keywords UBR5, siRNA, RNAi, Skeletal Muscle, Hypertrophy, Electroporation, MAPK, ERK, p90RSK, Akt, P70S6K, rpS6, eIF4e, PP2Ac.

Introduction

The regulation of skeletal muscle (SkM) mass is orchestrated by the activity of key signalling pathways that control protein breakdown and synthesis within myofibers. The breakdown or atrophy of SkM mass is mediated, in-part, by the ubiquitin-proteasome system (3, 7), which is composed of three key enzymes that activate and conjugate (E1 & E2 enzymes) small ubiquitin molecules to target protein substrates (E3 ligases) for recognition and subsequent degradation in the 26S proteasome. The most characterised E3 ubiquitin ligases associated with SkM atrophy are the muscle specific RING finger protein 1 (MuRF1 or Trim63) and the F-box containing ubiquitin protein ligase atrogin-1 (Atrogin-1; 16)), otherwise known as muscle atrophy F-box (MAFbx; 4).

Interestingly, recent work identified that a HECT domain E3 ligase named, ubiquitin protein ligase E3 component n-recognin 5 (EDD1 or UBR5) was significantly altered at the DNA methylation and gene expression level following resistance exercise (RE) in human SkM (32, 33). UBR5 DNA methylation decreased (hypomethylated) and mRNA expression increased after 7 weeks of training-induced SkM hypertrophy, with further enhanced changes reported following a later 7 weeks of retraining (32, 33). The pattern observed in DNA methylation and gene expression, which significantly correlated with changes in lean mass, suggested that there may be a role for UBR5 during muscle hypertrophy in contrast to E3 ligases, MuRF1 and MAFbx that are associated with atrophy. Additional work has provided further support for this hypothesis, whereby UBR5 expression significantly increased after acute mechanical loading in bioengineered SkM *in-vitro*, in response to synergistic ablation/functional overload (FO), and after programmed resistance training in rodent muscle *in-vivo,* yet with no change in MuRF1 and MAFbx expression (31). UBR5 also increased during recovery from hindlimb unloading (HU) and tetrodotoxin induced-disuse atrophy, again with no increase in MuRF1 and MAFbx (31). Furthermore, increased gene expression of UBR5 in these models resulted in greater abundance of UBR5 protein content following FO-induced hypertrophy of the mouse plantaris muscle *in-vivo*, and over the time-course of regeneration in primary human muscle cells *in-vitro* (31). A recent study also supported the role of UBR5 as being essential for muscle growth through RNAi screening in *Drosophila* larvae, where UBR5 inhibition led to smaller sized larvae (22). Collectively, these data support the notion that UBR5 is involved in load-induced anabolism and hypertrophy, in contrast with the well-known MuRF1 and MAFbx E3 ligases that are associated with muscle atrophy.

The most characterised signalling pathway involved in anabolism, protein synthesis and hypertrophy of SkM is the Akt/mTORC1/p70S6K pathway (Baar *et al.*, 2000; Bodine *et al.*, 2001;

Goodman *et al.*, 2011). Further work by the Esser laboratory also reported PI3K/Akt-independent activation of mTORC via mitogen-activated protein kinase (MEK)/extracellular signal-regulated kinase (ERK) signalling which was critical for overload-induced hypertrophy (27). Earlier work also demonstrated increased ERK1/2 phosphorylation after acute resistance exercise (RE) in humans (12) and after mechanical loading in C_2C_{12} myotubes (20). Downstream of ERK1/2, phosphorylation of the ribosomal S6 kinase (p90RSK) has been shown to increase with acute endurance and resistance exercise in rodent and human SkM (28, 38, 40). Interestingly, previous work also suggests that UBR5 is regulated via ERK/p90RSK signalling in non-muscle cells (9). Indeed, UBR5 has been shown to be a target substrate for ERK2 in the COS-1 kidney fibroblast cell line after treatment with epidermal growth factor (EGF), an established ligand that initiates downstream ERK signalling when bound to its receptor (EGFR) (14). Others have also shown that p90RSK, phosphorylates UBR5 in HeLa cancer cells at various sites, and may therefore be involved in growth of cancer cells (9). Further, UBR5 has been suggested to target protein phosphatase 2A subunit C (PP2Ac; catalytic subunit) for proteasomal degradation which is reported to negatively regulate Akt and ERK cascades (24–26, 34). Therefore, given that ERK/p90RSK signalling is associated with load-induced SkM hypertrophy (27) and UBR5 is associated with ERK/p90RSK signalling in non-muscle cells (9, 14), assessing ERK/p90S6K signalling as well as established load-induced Akt/ p70S6K signalling, together with negative regulator PP2Ac, after experimental manipulation of UBR5 is required to elucidate UBR5s mechanistic role in positively regulating muscle mass.

Therefore, in the present study, we knocked down UBR5 into murine tibialis anterior (TA) muscle using a miR-based RNAi via pcDNA TM 6.2-GW/EmGFP-miR to investigate the impact of reduced UBR5 on MEK/ERK/p90RSK/MSK1 and PP2Ac/Akt/GSK3β/p70s6K/rpS6/eIF4e signalling *in-vivo*, protein synthesis, fibre size and muscle mass. Given that increased UBR5 is associated with anabolism and hypertrophy, we hypothesised that knockdown of UBR5 would perturb ERK and Akt signalling pathways, reduce protein synthesis and result in muscle atrophy.

Methods

Skeletal Muscle Tissue

C57Bl/6 male mice between twelve and sixteen weeks-old (*n* = 10/time point) were obtained from Charles River Laboratories for electroporation experiments. Animals were housed in ventilated cages maintained in a room at 21 °C with 12-h light/ dark cycles and had ad libitum access to standard chow (Harlan-Teklad 190 formula 7913) and water throughout the study. All animal

procedures were approved by the Institutional Animal Care and Use Committee at the University of Iowa. During tissue collection, animals were anaesthetized with 2–3% inhaled isoflurane. On completion of tissue removal, mice were euthanised by exsanguination.

Plasmid Design and Electroporation of Skeletal Muscle Tissue In-Vivo

An RNAi system which was designed and purchased from Invitrogen (Thermo Fisher Scientific, *USA*) was implemented. Specifically, the negative control/empty vector (EV) RNAi plasmid was described previously (13, 21, 31) and encodes emerald green fluorescent protein (EmGFP) and a non-targeting pre-miRNA under bicistronic control of the CMV promoter in the pcDNA6.2GW/EmGFP-miR plasmid (Invitrogen). The UBR5 RNAi plasmid also encodes EmGFP plus an artificial pre-miRNA targeting mouse UBR5 under bicistronic control of the CMV promoter. It was generated by ligating the Mmi571982 oligonucleotide duplex (Invitrogen) into the pcDNA6.2GW/EmGFP-miR plasmid. The UBR5 RNAi plasmid is designed to target the nucleotide sequence in the HECT domain between amino acids positions 2695-2754 (location/schematic of the RNAi on UBR5 protein structure is also included in the results). The electroporation technique was performed as previously described (31). Briefly, after a 2hr pre-treatment with 0.4 units/ul of hyaluronidase, 20 μg plasmid DNA was injected into the tibialis anterior (TA) muscle and the hind limbs were placed between two-paddle electrodes and subjected to 10 pulses (20 msec) of 175 V/cm using an ECM-830 electroporator (BTX Harvard Apparatus). Using a within-animal experimental design, mice were injected with the UBR5 RNAi plasmid and an empty vector (EV) control into the contralateral muscle. TA muscles were harvested after 7 and 30 days.

Skeletal Muscle Tissue Collection

Following completion of the appropriate time period, mice were anesthetized with isoflurane, and the TA muscles were excised, weighed, frozen in liquid nitrogen, and stored at −80°C for later analyses. Muscles were collected for histology (n = 5/time point) and RNA/Protein isolation (n = 5/time point) and processed as described below. On completion of tissue removal, mice were euthanized by exsanguination.

Immunohistochemistry and Histology

Harvested mouse TA muscles were immediately weighed and fixed in 4% (w/v) paraformaldehyde for 16 h at 4˚C and then placed in 30% sucrose for overnight incubation. The TA muscles were then embedded in Tissue Freezing Medium (Triangle Biomedical Sciences), and a Thermo HM525 cryostat

was used to prepare 10 µm sections from the muscle mid-belly. All sections were examined and photographed using a Nikon Eclipse Ti automated inverted microscope equipped with NIS-Elements BR digital imaging software.

Laminin Staining

TA muscle sections were permeabilized in PBS with 1% triton for 10 minutes at room temperature. After washing with PBS, sections were blocked with 5% goat serum for 15 minutes at room temperature. Sections were incubated with Anti-Laminin (1:500, Sigma-Aldrich Cat# L9393, RRID: AB_477163) in 5% goat serum for 2 hours at room temperature, followed by two 5-minute washes with PBS. Goat-anti-rabbit AlexaFluor® 555 secondary (1:333, Invitrogen Cat# A28180, RRID: AB_2536164) in 5% goat serum was then added for 1 hour at room temperature. Slides were cover slipped using ProLong Gold Antifade reagent (Life Technologies). Image analysis was performed using Myovision software (36). Skeletal muscle fiber size was analyzed by measuring ≥ 250 transfected muscle fibers per muscle, per animal (10x magnification). Transfected muscle fibers were identified as GFP-positive as shown in results figures for 7 days and 30 days. We also measured the size of non-transfected fibers (GFP-negative) from the transfected muscles at all time points. Comparison of the CSA distributions of GFP-negative fibers in EV and UBR5 RNAi transfected muscles revealed no difference between groups. Therefore, fiber size comparisons were made between the GFP-positive fibers in the EV controls and UBR5 RNAi transected muscles.

RNA Isolation and Total RNA Quantification

Prior to RNA isolation, aliquots of frozen muscle powder were weighed in order to calculate RNA per milligram of wet muscle tissue. Muscle powder was homogenized using RNAzol RT reagent (Sigma-Aldrich, St Louis, MO) in accordance with the manufacturer's instructions. Total RNA quantity and quality was assessed for 260/280 ratios using a SpectraMax M2 Microplate reader (Molecular Devices, CA, USA).

Muscle Protein Synthesis (MPS)

Changes in MPS were assessed in TA muscles transfected for 7 days by measuring the incorporation of exogenous puromycin into nascent peptides as described previously (18, 37). Puromycin (EMD Millipore, Billerica, MA, USA; cat. no. 540222) was dissolved in sterile saline and delivered (0.02 µmol g^{-1} body weight by I.P. injection) 30 min prior to muscle collection. Protein synthesis was measured under fed conditions and studied in the light cycle.

Immunoblotting

Frozen TA muscles were homogenized in sucrose lysis buffer (50 mM Tris pH 7.5, 250 mM sucrose, 1 mM EDTA, 1 mM EGTA, 1% Triton X 100, 50 mM NaF). The supernatant was collected following centrifugation at 8,000 *g* for 10 minutes and protein concentrations were determined using the 660-protein assay (Thermo Fisher Scientific, Waltham, MA). Twelve micrograms of protein were subjected to SDS-PAGE on 4-20% Criterion TGX stain-free gels (Bio-Rad, Hercules, CA) and transferred to polyvinylidene diflouride membranes (PVDF, Millipore, Burlington, MA). Membranes were blocked in 3% nonfat milk in Tris-buffered saline with 0.1% Tween-20 added for one hour and then probed with primary antibody (concentrations detailed below) overnight at 4°C. Membranes were washed and incubated with HRP-conjugated secondary antibodies at 1:10,000 (Mouse, Cell Signaling technology, RRID AB_330924; Rabbit, Cell Signaling technology, RRID AB_2099233) for one hour at room temperature. Immobilon Western Chemiluminescent HRP substrate was then applied to the membranes prior to image acquisition. Image acquisition and band quantification were performed using the Azure C400 System (Azure Biosystems, Dublin, CA, USA) and Image Lab, version 6.0.1 (Bio-Rad), respectively. Total protein loading of the membranes captured from images using stain-free gel technology was used as the normalization control for each phosphorylated and total protein analyte. For phosphorylated to total protein ratios, normalized phosphorylation values were divided by total normalized values. The following primary antibodies were used all used at a concentration of 1:1000: Cell Signaling Technologies (Danvers, MA, USA) – phospho-ERK1/2 $^{Thr202/Tyr204}$ (RRID:AB_2315112), ERK1/2 (RRID:AB_390779), phospho-p90RSK ^{Ser380} (RRID:AB_2687613), p90RSK (RRID:AB_659900), phospho-MSK1 ^{Thr581} (RRID:AB_2181783), phospho-MEK1/2 $^{Ser217/221}$ (RRID:AB_2138017), phospho-Akt ^{Ser473} (RRID:AB_2315049), Akt (RRID:AB_329827), phospho-GSK3β ^{Ser9} (RRID:AB_331405), GSK3β (RRID:AB_2335664), phospho-p70S6K Thr^{389} (RRID:AB_330944), p70S6K (RRID:AB_331676), phospho-rpS6 $^{Ser240/244}$ (RRID:AB_10694233), rpS6 (RRID:AB_331355), phospho-4EBP1 $^{Thr37/46}$ (RRID: AB_560835), 4EBP1 (RRID:AB_2097841) UBR5 (RRID:AB_2799679), PP2Ac (RRID:AB_561239), eIF4e (RRID:AB_823488) and EMD Millipore – puromycin (RRID:AB_2566826). Knockdown of UBR5 protein was confirmed previously with a reduction of 65% (± 11.8%) (Seaborne *et al.*, 2019) and all signaling antibodies in the present study were processed on the same samples as this UBR5 protein data.

Statistical Analysis

Paired *t-tests* were carried out when comparing empty control (EV) vs. UBR5 RNAi transfected mouse TA. All statistical analysis was performed using GraphPad Software (Prism, Version 7.0a, San

Diego, CA). Data is presented as means ± standard error of the mean (SEM). $P \leq 0.05$ represents statistical significance.

Results

Fiber CSA was significantly reduced at 7 days post UBR5 RNAi electroporation in mice

To examine the effect of reducing UBR5 expression *in-vivo*, mouse TA muscles were transfected with either UBR5 RNAi plasmid targeting UBR5s HECT domain (Figure 1A) or an EV control. UBR5 protein was significantly reduced by 65% (± 11.8%) in UBR5 RNAi conditions (Figure 1B), as previously demonstrated (31). The TA mass (mg) did not significantly change at 7 days post electroporation in UBR5 RNAi vs. EV transfected TA muscle (Figure 1C). However, measurement of the CSA of GFP-positive fibers revealed that the mean fiber CSA of GFP-positive fibers was significantly reduced (-9.5 ± 3.2%) in RNAi transfected TA muscle ($P = 0.048$; Figure 1D & E) with fewer larger fibers (≥3400 μm^2) present versus the EV (Figure 1D & F).

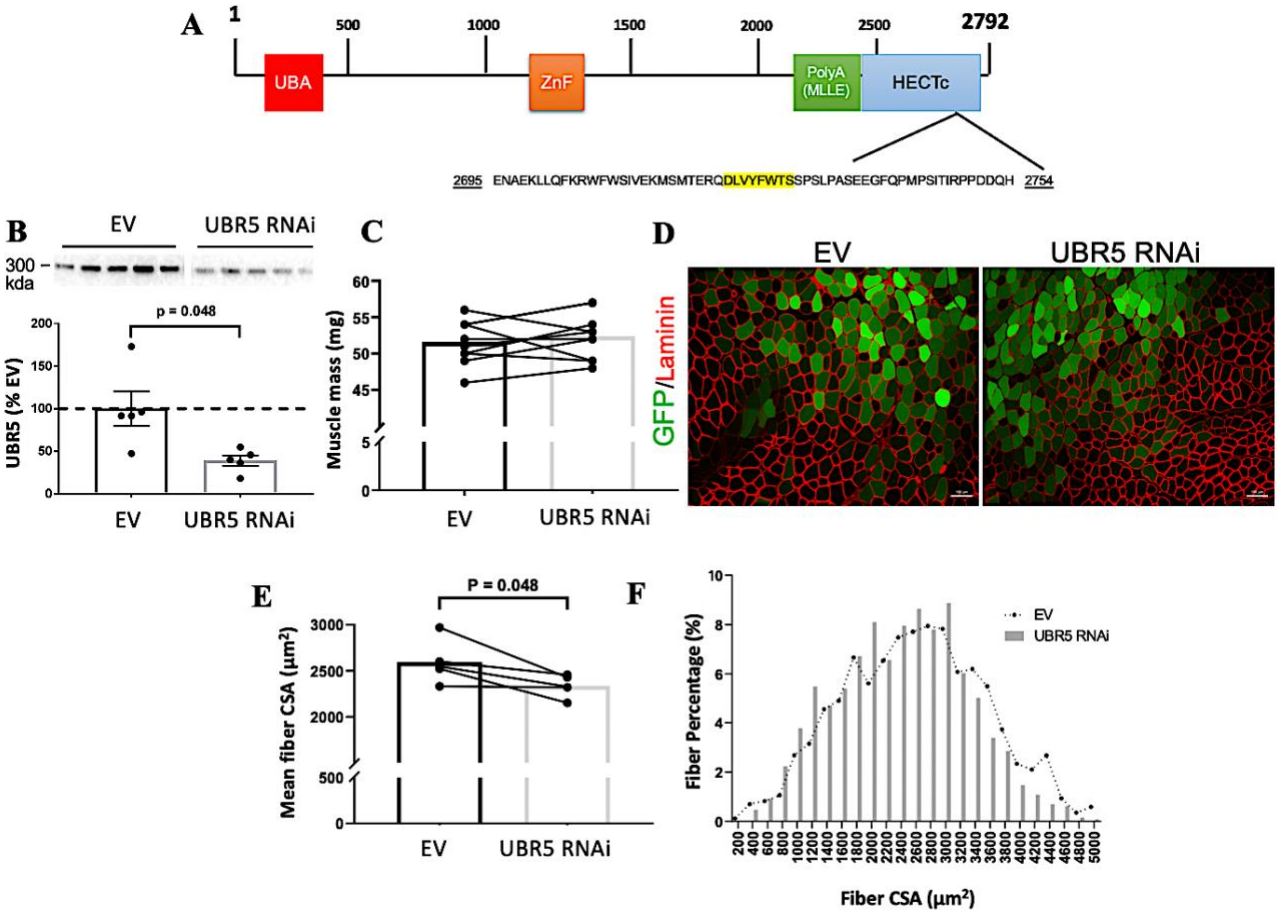

Figure 1. Characteristics of tibialis anterior muscle mass and fiber CSA in UBR5 RNAi transfected TA muscle after 7 days. (A) Schematic/ putative domain structure of UBR5 protein consisting of ubiquitin-associated (UBA) domain-like superfamily, Putative zinc finger in N-recognin (ZnF), Poly-adenylate binding protein (PolyA), MLLE protein/protein

interaction domain and a HECT domain. The UBR5 RNAi plasmid was designed to target the nucleotide sequence in the HECT domain between amino acids position 2695-2754 (highlighted in yellow in A). **(B)** Reduction of UBR5 protein levels by 65% (Seaborne et al., 2019) in UBR5 RNAi conditions at 7 days. We have previously confirmed significant reductions in UBR5 protein levels at 7 days with this UBR5 RNAi plasmid (Seaborne et al., 2019), and all 7 day data in the present manuscript (muscle mass (C), histology (D), fiber CSA (E) RNA and signaling data – figures below) are analyzed from the same animals/samples as this UBR5 protein data. Figure 1B is therefore reused with permissions from; R. A. Seaborne et al., *Journal of Physiology* (Wiley), 597.14 (2019) pp 3727–3749, Copyright-2019 The Authors. *The Journal of Physiology*. Copyright-2019 The Physiological Society). **(C)** Muscle mass between empty vector control (EV) and UBR5 RNAi transfected TA muscles (*n* = 10 per group). **(D)** Representative images (10x magnification; scale bar = 100 µm) for GFP transfected fiber identification and CSA quantification through laminin staining. **(E)** Mean transfected fiber CSA size in the RNAi transfected vs. EV muscles *(n* = 5 per group). **(F)** Quantification of muscle CSA revealed changes in the percentage of large fibers (≥3400 μm^2) with RNAi transfected muscles verses the EV group (n = 5 per group). Statistical significance is depicted where present (P ≤ 0.05).

Total RNA concentrations, muscle protein synthesis, ERK1/2 and Akt activity and total p90RSK are reduced in UBR5 RNAi TA muscle after 7 days

Along with a reduction in fiber CSA at 7 days post UBR5 RNAi, a significant reduction in total RNA concentrations (*P* = 0.01, Figure 2A) and protein synthesis (-17 ± 3.2%, *P* = 0.05, Figure 2B & 3C) was evident. Wishing to determine potential regulators of this process in the ERK signalling pathway (Figure 2D), ERK1/2 (p44/42 MAPK) was examined and its phosphorylation found to be reduced (-43 ± 2.3%, *P* = 0.03, Figure 2E). When calculating ERK1/2 total levels there was also a reduction, albeit non-significant (Figure 2F) making the phosphorylation to total activity ratio of ERK1/2 unchanged (Figure 2G). Interestingly, the reduction in RNA, protein synthesis and ERK1/2 phosphorylation coincided with a significant increase in phospho-p90RSK^{Ser380} (170 ± 39.8%, *P* = 0.04; Figure 2H) at 7 days. This was on the background of a significant 45% decrease in total p90RSK (-45 ± 5.6%, P = 0.02; Figure 2I), resulting overall in an increased phosphorylation / total activity ratio for p90RSK (0.83 ± 0.1 EV vs. 2.57 ± 0.6 UBR5 RNAi, P = 0.04, Figure 2J). We also observed no differences in the phosphorylation of MEK 1/2$^{Ser\ 217/221}$ or MSK-1^{Thr581} between RNAi and EV transfected TA muscles after 7 days (data not depicted). We next assessed protein signalling associated with the Akt pathway (Figure 3A). As with ERK1/2, there were significant reductions in Akt ^{ser473} phosphorylation (-26 ± 9%, P = 0.03; Figure 3B), with no changes in total levels of Akt (Figure 3C) and therefore significant reductions in Akt phosphorylation activity ratio (1.37 ± 0.1 EV vs. 1.15 ± 0.2 UBR5 RNAi, P = 0.04, Figure 3D). There were also significant reductions in GSK-3β ^{Ser9} phosphorylation to total ratio after 7 days post-electroporation (1.60 ± 0.1 EV vs. 1.32 ± 0.2

UBR5 RNAi, P = 0.03, Figure 3E, F, G). Interestingly, despite reductions in ERK1/2 phosphorylation, Akt and protein synthesis, we observed significant elevations in phosphorylation for p70S6K ^{Thr389} (176 ± 57%, P = 0.02; Figure 3H), with no changes in its total levels (Figure 3I) and therefore significantly increased phosphorylation to total ratios (2.62 ± 0.9 EV vs. 5.4 ± 1.7 UBR5 RNAi, P = 0.02, Figure 3J). The same trend was observed for rpS6 $^{Ser240/244}$ with increases in its phosphorylation (178 ± 39.4%, P = 0.01; Figure 4K), no change in its total (Figure 3L) and thus an increase in its activity ratio (1.62 ± 0.3 EV vs. 2.82 ± 0.3 UBR5 RNAi, P = 0.01, Figure 3M) in UBR5 RNAi transfected muscles at 7 days. Furthermore, no reduction in 4E-BP1 $^{Thr37/46}$ phosphorylation levels (Figure 3N), yet a significant reduction in its total levels (Figure 3O), resulted in a significant reduction in its activity ratio (0.68 ± 0.01 EV vs. 0.84 ± 0.05 UBR5 RNAi, P = 0.01, Figure 3P). Finally, there were no changes to total protein levels of eIF4e or PP2Ac at 7 days in UBR5 RNAi transfected muscles (Figure 3Q & 4R respectively).

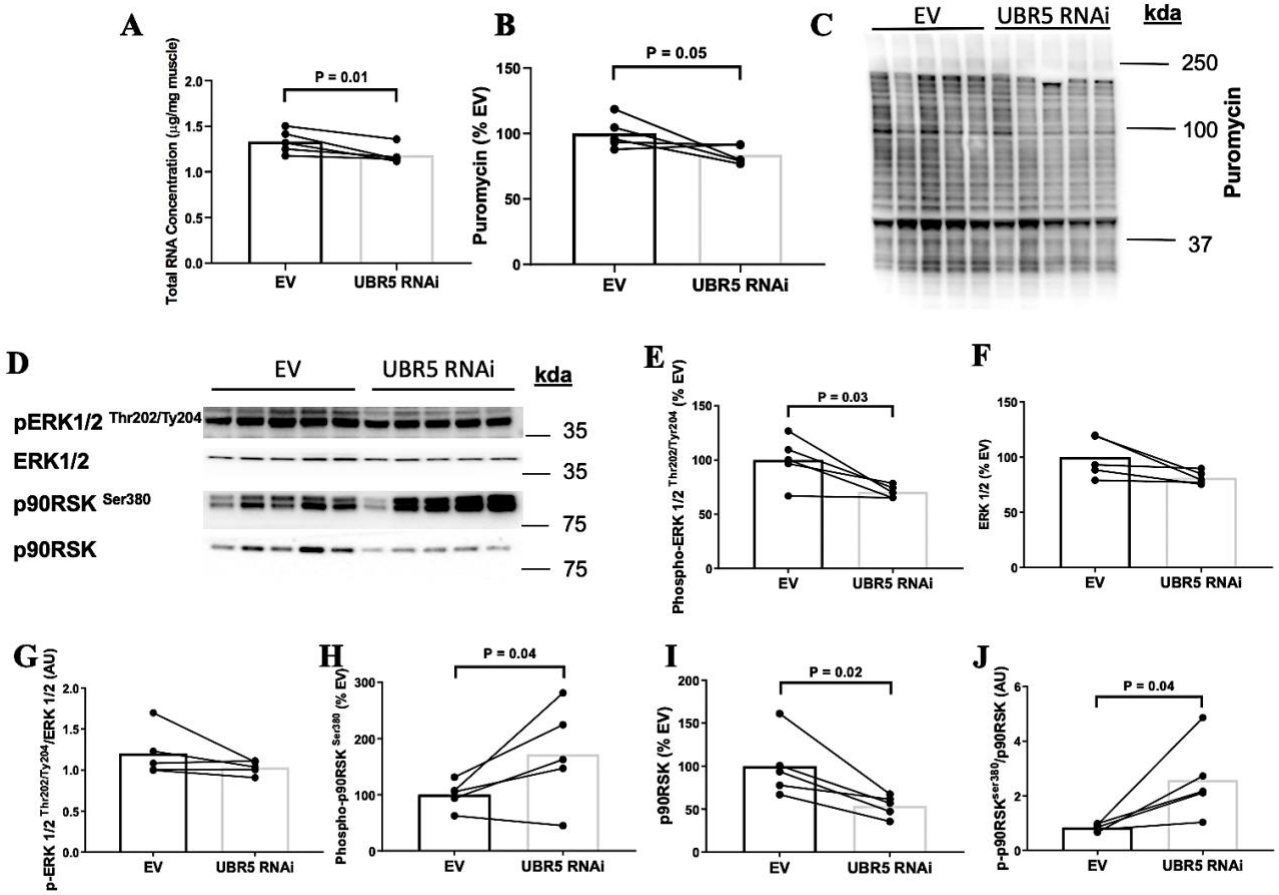

Figure 2. Alteration in total RNA, protein synthesis and MAPK (ERK/p90RSK) signaling in UBR5 RNAi transfected TA muscle after 7 days. (A) Total RNA concentration, **(B & C)** muscle protein synthesis (B) assessed via western blots for puromycin incorporation (C). **(D)** Western blot images for the ERK signaling pathway. **(E)** Phosphorylation levels of ERK1/2 (p44/42 MAPK), **(F)** total levels of ERK1/2, **(G)** phosphorylation to total activity ratio of ERK1/2. **(H)** Phosphorylation levels of p90RSK, **(I)** total levels of p90RSK (*P* = 0.02), and **(J)** phosphorylation to total p90RSK activity

ratio.. Total protein loading of the membranes captured from images using stain-free gel technology was used as the normalization control. N = 5 per group. Statistical significance is depicted where present (P ≤ 0.05).

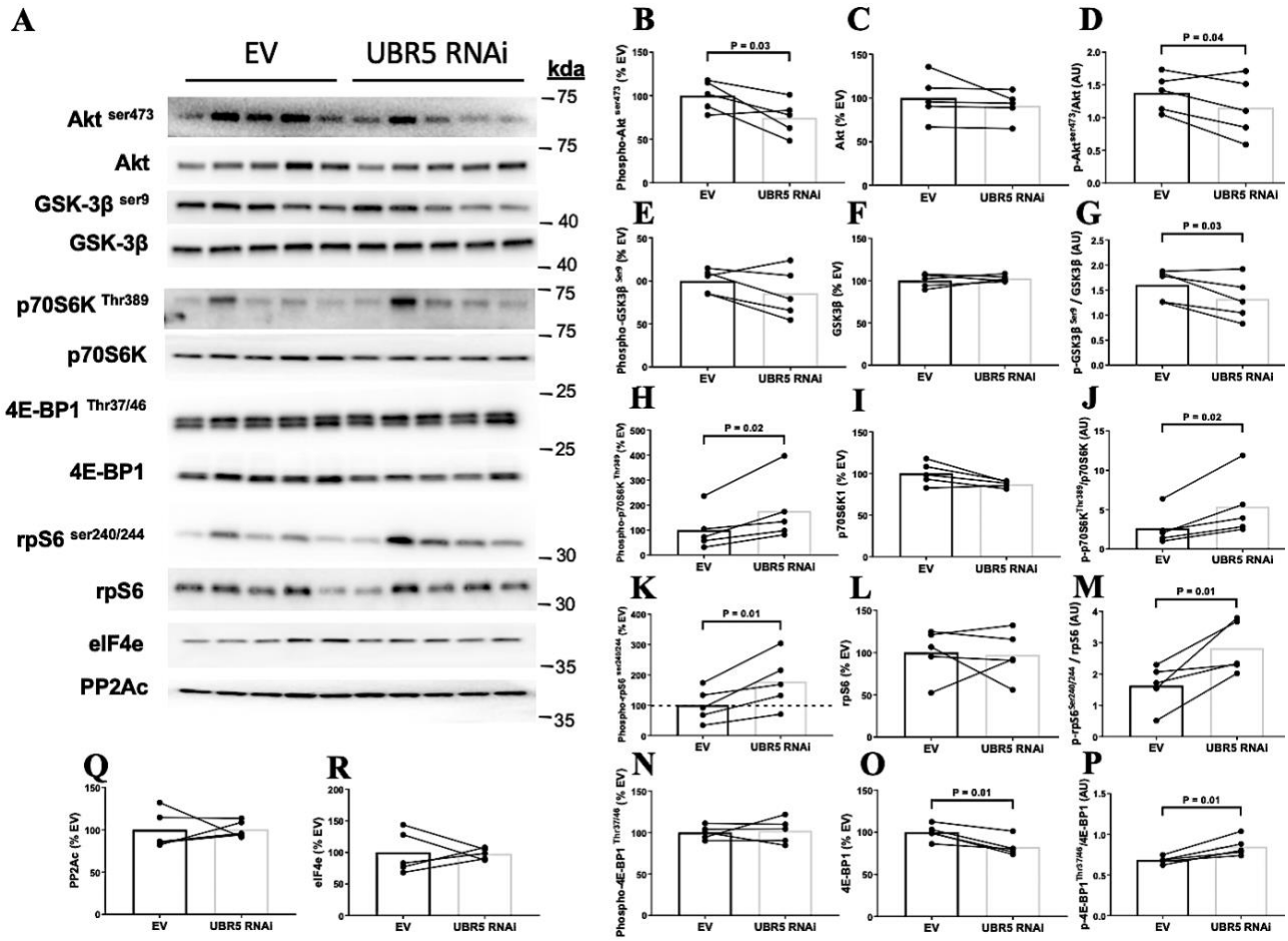

Figure 3. (A) Western blot analysis for the Akt signaling pathway (Akt, GSK-3β, p70S6K, 4E-BP1, rpS6, eIF4e, PP2Ac) in UBR5 RNAi transfected TA muscle after 7 days. (B-P) Phosphorylation, total levels and phosphorylation / total ratios respectively for Akt **(B-D)**, GSK-3β **(E-G)**, p70S6K **(H-I)**, rpS6 **(K-M)**, 4E-BP1 **(N-P)**. **(Q)** PP2Ac protein levels**,** and **(R)** eIF4e levels. All *n* = 5 per group – EV control and UBR5 RNAi. Total protein loading of the membranes captured from images using stain-free gel technology was used as the normalization control. Statistical significance is depicted where present (P ≤ 0.05).

Prolonged UBR5 RNAi transfection leads to significant loss of muscle mass and fiber CSA atrophy in mouse skeletal muscle

Given the data over 7 days, the next question to interrogate was the impact of UBR5 RNAi transfection in TA muscle after a prolonged period (30 days), with the hypothesis that this would perhaps lead to greater muscle atrophy vs. 7 days of UBR5 suppression. In line with this hypothesis, while UBR5 protein reductions were not maintained out to this 30-day timepoint (Figure 4A), the earlier reductions in UBR5 at 7 days led to a significant reduction in muscle mass by 30 days (-4.6 ± 1.5%) in UBR5 RNAi transfected vs. EV muscles (P = 0.01; Figure 4B). Alongside the reduction in muscle mass, a significant larger reduction in GFP-positive fiber CSA (-18.2 ± 2.3% at 30 d vs. -9.5 ±

3.2% at 7 d) was evident after UBR5 RNAi transfection (P = 0.01; Figure 4C & D) vs. EV control, with the RNAi transfected muscles displaying a shift in the distribution of fiber CSA primarily towards smaller fibers (≥ 2600 µm^2) compared to the EV control muscle (Figure 4E). These observations provide further support towards UBR5 being a positive modulator of muscle mass, with its knockdown evoking considerable atrophy.

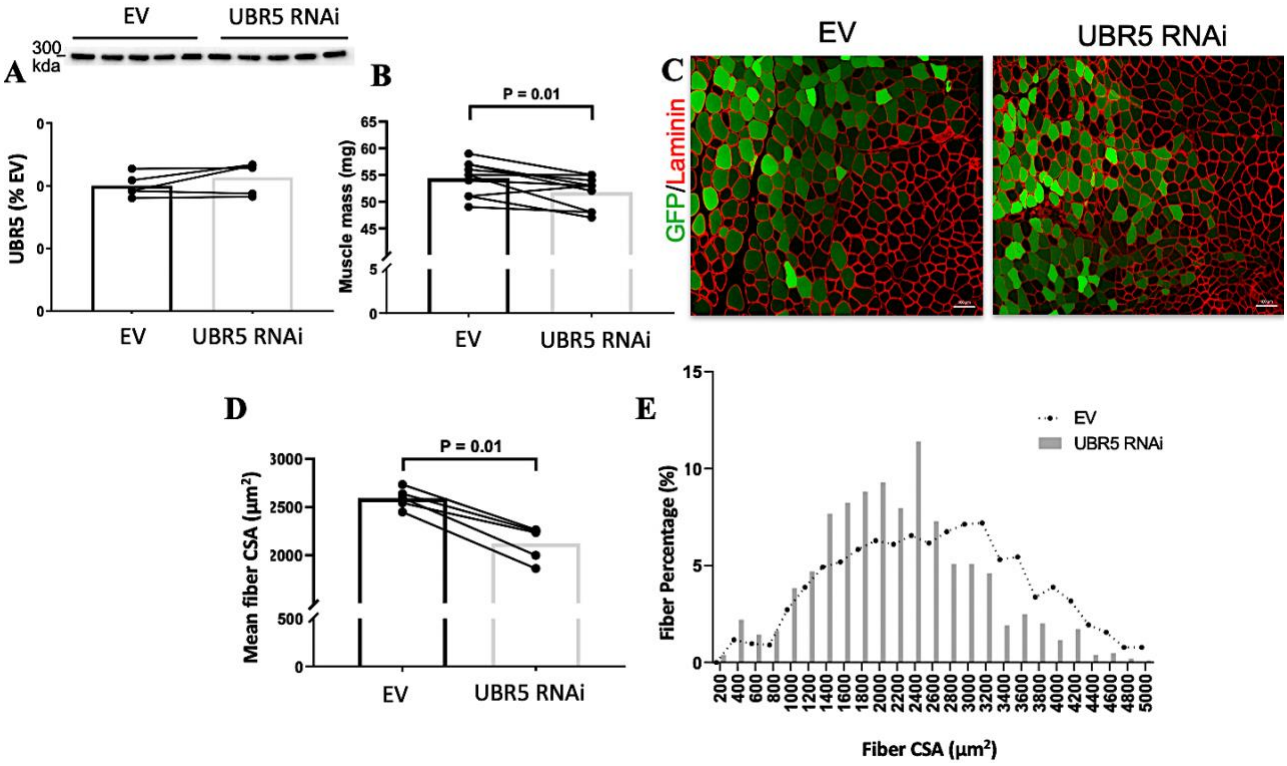

Figure 4. Loss of muscle mass and fiber CSA in UBR5 RNAi transfected TA muscle after 30 days. (A) UBR5 protein after 30 d UBR5 RNAi. (**B)** After 30 days, muscle mass was significantly reduced in UBR5 RNAi transfected vs. empty vector control (EV) TA muscles (P = 0.01; *n* = 10 per group). **(C)** Representative images (10x magnification; scale bar = 100 µm) for GFP transfected fiber identification and CSA quantification through Laminin staining. **(D)** A significant reduction (*P* = 0.01) in mean transfected fiber CSA size was observed in the RNAi transfected vs. EV muscles *(n* = 5 per group). **(E)** Quantification of transfected muscle CSA revealed a leftward shift from large to smaller fiber sizes (≥3400 µm^2) with RNAi transfected muscles verses EV group (**D**). Statistical significance is depicted where present (P ≤ 0.05).

Prolonged UBR5 RNAi at 30 days and reductions in muscle mass and fiber size are associated with increased PP2Ac, reduced eIF4e and inappropriate chronic elevation of p70S6K and rpS6

At 30 days post RNAi transfection phosphorylated ERK1/2 was significantly increased (Figure 5A), as were its total levels (Figure 5B) resulting in no significant change in its activity ratio (Figure 5C). A similar trend was observed for p90RSK (Figures 5D, E, F). As with 7 days, we observed no differences in the phosphorylation of MEK 1/2$^{Ser\ 217/221}$ or MSK-1^{Thr581} between RNAi and EV transfected TA muscles after 30 days (data not depicted). For the Akt signalling pathway (Figure 6A), by 30 days there was no reduction of phosphorylated Akt (Figure 6B, C, D) as observed at the 7-day timepoint.

However, there was a continued reduction in GSK-3β phosphorylation with RNAi transfection (Figure 6E, F, G). Interestingly, elevation of p70S6K and rpS6 phosphorylation from the 7-day time point continued over the more chronic period of 30 days, demonstrating a 4- and 2-fold increase respectively in the RNAi transfected muscles verses the empty vector control group (Figure 6H, I, J and 6K, L, M respectively). There were no changes in activity of 4E-BP1 $^{Thr37/46}$ in UBR5 RNAi transfected muscles at 30 days (Figure 6N, O, P). Compared to the 7d time point, we also observed an 80% reduction in eIF4e protein levels in the RNAi group (Figure 6Q). Furthermore, the levels of PP2Ac were significantly increased at the 30 day time point (Figure 6R). Signalling events at 7 and 30 days are summarised in the cell signalling diagram (Figure 7).

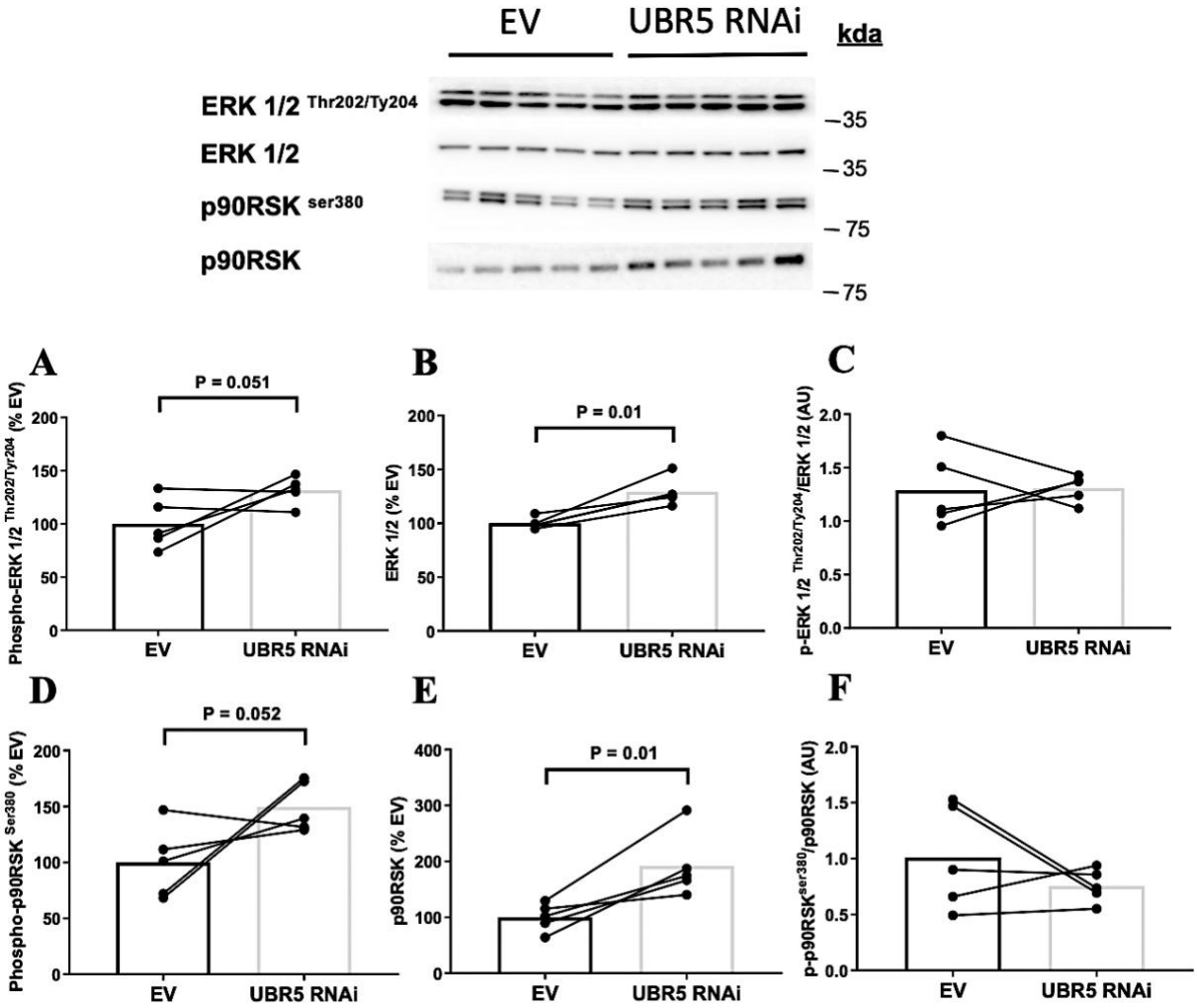

Figure 5. ERK pathways signaling in UBR5 RNAi transfected TA muscle after 30 days. (A) Phosphorylated ERK1/2, **(B)** total ERK1/2, **(C)** ratio of phosphorylated ERK1/2 to total ERK1/2. **(D)** Phosphorylated p90RSK, **(E)** total p90RSK, **(F)** ratio of phosphorylated p90RSK to total p90RSK. All *n* = 5 per group – EV control and UBR5 RNAi. Total protein loading of the membranes captured from images using stain-free gel technology was used as the normalization control. Statistical significance is depicted on figures where present (P ≤ 0.05).

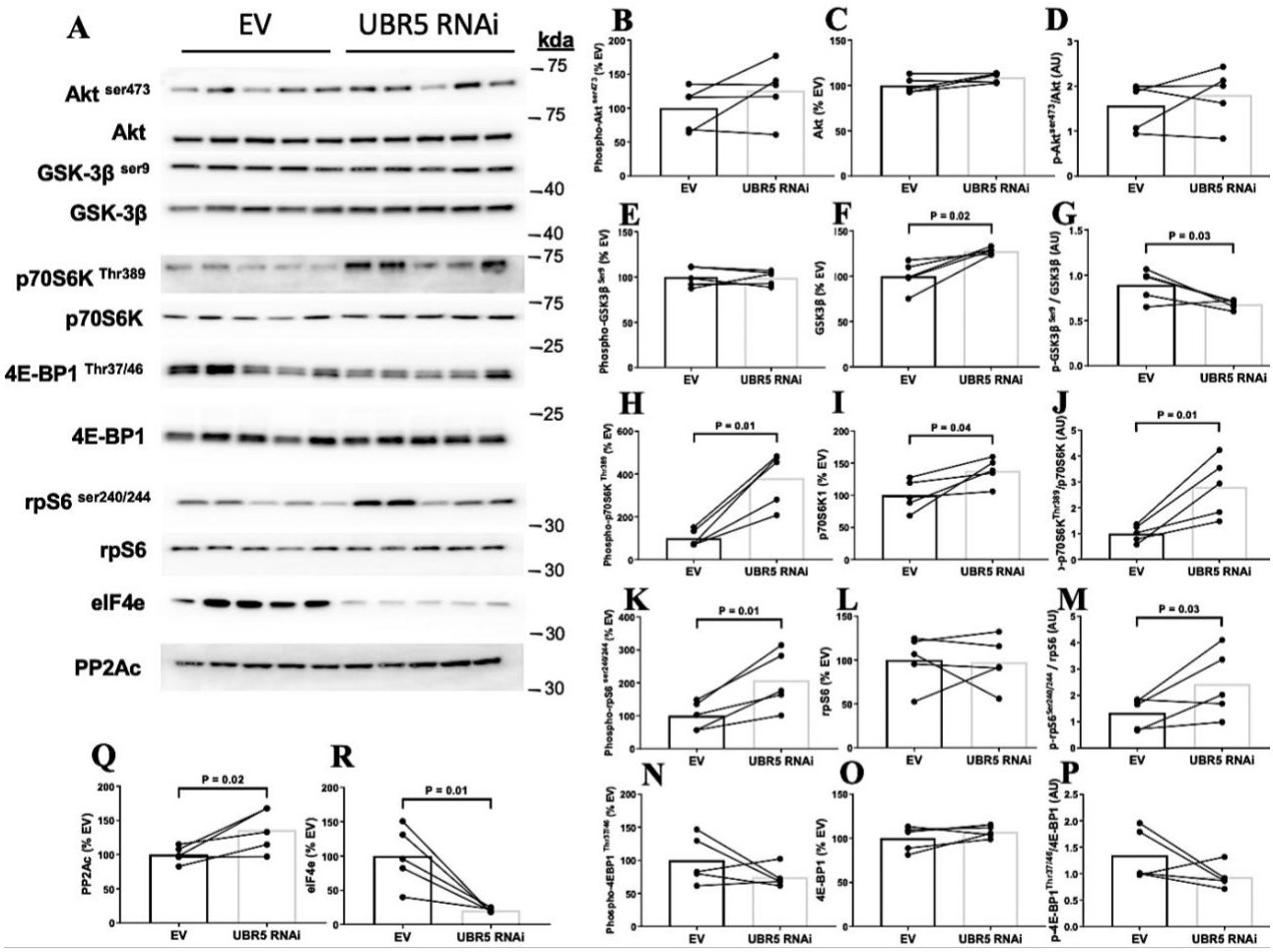

Figure 6. (A) Western blot analysis for the Akt signaling pathway (Akt, GSK-3β, p70S6K, 4E-BP1, rpS6, eIF4e, PP2Ac) in UBR5 RNAi transfected TA muscle after 30 days. (B-P) Phosphorylation, total levels and phosphorylation / total ratios respectively for Akt **(B-D)**, GSK-3β **(E-G)**, p70S6K **(H-I)**, rpS6 **(K-M)**, 4E-BP1 **(N-P)**. **(Q)** PP2Ac protein levels, and **(R)** eIF4e levels. All *n* = 5 per group – EV control and UBR5 RNAi. Total protein loading of the membranes captured from images using stain-free gel technology was used as the normalization control. Statistical significance is depicted where present ($P \leq 0.05$).

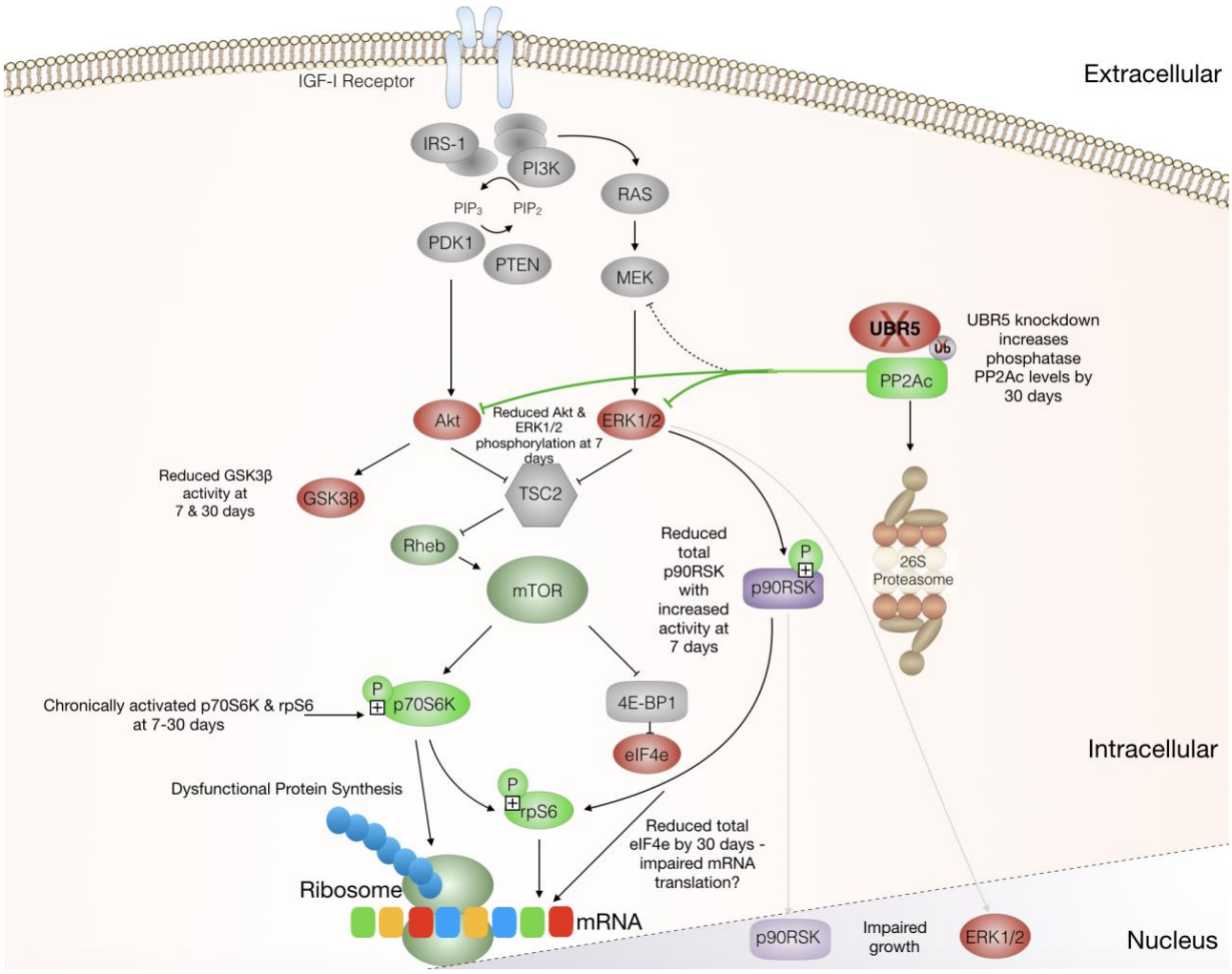

Figure 7. Schematic of cell signaling events after UBR5 knockdown in skeletal muscle in-vivo. UBR5 knockdown (X) increases phosphatase PP2Ac by 30 days; reduces ERK1/2, Akt phosphorylation at 7 days and GSK-3β activity at 7 and 30 days (RED); reduces total p90RSK at 7 days and eIF4e at 30 days (PURPLE); chronically increases the phosphorylation of p70S6K and rpS6 (GREEN).

Discussion

The present study aimed to investigate the impact of reduced UBR5 on ERK and Akt signalling pathways in SkM tissue using our miR-based RNAi for UBR5 electroporated into the tibialis anterior (TA) of mice. Indeed, transfection of UBR5 RNAi into the TA muscle of mice after 7 days caused a significant reduction in fiber CSA, total RNA, global protein synthesis and ERK1/2, Akt phosphorylation and GSK3β activity. However, p90RSK, P70S6K and rps6 phosphorylation significantly increased, perhaps suggestive of a potential compensatory mechanism triggered by the reduction in UBR5 or inappropriate chronic activation of these pathways, like that observed in aged muscle (discussed below). Furthermore, the increases in p90RSK phosphorylation were on a background of considerably reduced total p90RSK levels. Finally, the changes observed above at 7 days culminated in further reductions in muscle mass and fiber CSA after prolonged (30 days) UBR5

RNAi. This was associated with increased PP2Ac and, as hypothesised above, continued chronic elevation of P70S6K and rpS6 from 7 to 30 days, as well as reductions in elongation initiation factor 4e (eIF4e). Overall, the present study further supports the notion that UBR5 plays an important role in muscle anabolism and hypertrophy, and its reduction culminates in atrophy.

Electroporation of UBR5 RNAi for 7 days also induced a significant reduction in average myofiber CSA, frequency of larger myofibers (≥3400 μm^2), total RNA and muscle protein synthesis (~17%). The reduction in total RNA and muscle protein synthesis is interesting given the classification of UBR5 as an E3 ubiquitin ligase and thus its role in the ubiquitin-proteasome system. Indeed, UBR5 may have unidentified functions within skeletal muscle that are unrelated to proteasomal degradation. An example of an E3 ubiquitin ligase having other functions in skeletal muscle is TRIM72 (known as MG53), with its role being studied in cell membrane repair (6, 10, 11). UBR5 has been suggested to have a role in the regulation of mRNA translation and gene regulation through the MLLE domain on the UBR5 protein structure (29, 39). Recent studies have identified the translation capacity and activity of skeletal muscle to be important for growth and hypertrophy in rodent and human models (19, 30, 35, 37). Therefore, while we saw reductions in ERK/ Akt phosphorylation in the present study, there were opposite increases in p90RSK, p70S6K and rps6 suggesting that the observed reductions in protein synthesis may not be regulated by p90RSK, p70S6K and rps6 activity. However, there were significant reductions in total p90RSK as a consequence of UBR5 knockdown at 7d, that may contribute to the reductions in protein synthesis observed. However, given the observed reduction in total RNA, there could be a role for UBR5 in the regulation of mRNA translational capacity that would in-turn lead to reductions in total protein synthesis and skeletal muscle mass. Indeed, supporting this notion, we also observed 80% reductions of eiF4e at 30 days, an elongation initiation factor important for enhanced RNA translational efficiency, splicing and stability.

Other explanations for increased p90RSK, p70S6K and rpS6 signalling activity significantly increasing following UBR5 knockdown, are perhaps due to a compensatory or protective mechanism in an attempt to prevent the reductions in protein synthesis. Further, in a non-classically envisaged pathway, the increase in p90RSK activity may be explained due to its suggested role as an upstream regulator of UBR5 and its activation could therefore be altered due to the suppression of UBR5 protein levels (9). This could suggest that loss of UBR5 may indirectly lead to activation of p90RSK because its normal target for action is no longer present. Alongside the alterations in p90RSK

phosphorylation, as suggested above, we did observe a significant loss in total protein levels for p90RSK at 7 days which may contribute towards the alterations in p90RSK activity and the overall reductions in protein synthesis. There are currently no commercial antibodies to assess UBR5 activity in relation to p90RSK, something that warrants investigation when antibodies are developed in the future. In addition to alterations in ERK and Akt phosphorylation and reduced total p90RSK and protein synthesis at 7 days, a prolonged time period after transfection of the UBR5 RNAi at 30 days resulted in greater reductions in both muscle mass and fiber CSA. The loss of muscle mass and fiber size at 30 days was surprisingly accompanied by increased p70S6K and rpS6 phosphorylation. The chronic activation of mTORC/P70S6K signalling has been observed to be detrimental in skeletal muscle homeostasis, such as that with increasing age (2, 8, 23, 34). Therefore, subsequent future studies will seek to address the interplay between UBR5 and Akt/mTORC/p70S6K signalling with aging.

Finally, in the present study we observed significant increases in PP2Ac levels at 30 d RNAi. PP2Ac is a phosphatase demonstrated to inhibit Akt and ERK signalling, and importantly, UBR5 in its capacity as an ubiquitin ligase has been demonstrated to target PP2A for degradation in non-muscle studies (24–26, 34). While observing an increase in PP2Ac at 30 days, the reductions in phosphorylation of Akt and ERK were observed at 7 days and not at 30 days. However, the data does suggest for the first time in skeletal muscle, that PP2A is perhaps a target of UBR5 and that knockdown of UBR5 leads to an increase in the levels of PP2A due to a potential decrease in its degradation. However, UBR5 and its protein targets remain to be elucidated in skeletal muscle and require further study given these interesting findings.

Despite the exciting and novel findings surrounding UBR5's mechanistic role in skeletal muscle, it is worth acknowledging the limitations of the study, where UBR5 protein levels were not reduced at 30 d to the same degree as the 7d time point and this may be reflective of the effectiveness of the RNAi construct being reduced and also the influence of non-transfected muscle fibers in the biochemical analyses. However, the earlier reductions in UBR5 at 7 days still evoked altered signalling and greatest loss of muscle mass by this 30-day timepoint. Suggesting the earlier reductions in UBR5 at 7 days still culminated in later atrophy by 30 days. Lastly, it would also be prudent in future experiments to also evoke hypertrophy (e.g. via synergistic ablation) in rodents in the presence or absence of the UBR5 RNAi plasmid.

Conclusion

The present study supports the notion that UBR5 plays an important role in muscle anabolism/hypertrophy, and presents novel findings demonstrating knockdown of UBR5 is associated with early reductions in ERK1/2 and Akt phosphorylation and GSK3β activity, total p90RSK and protein synthesis that culminates in later atrophy that is associated with increased PP2Ac, reduced eIF4e levels and inappropriately chronically elevated activity of p70S6K and rpS6.

Author contributions

DCT, DCH, LMB, SCB, APS conceived and designed the research. All authors were involved in acquisition or analysis or interpretation of data for the work. DCT, DCH, LMB, SCB, APS drafted the work. All Authors were involved in revising the work critically for important intellectual content. All authors approved the final version of the manuscript.

Funding

DCT was funded via PhD studentships from Keele University and Liverpool John Moores University (LJMU) via APS. DCTs project was further supported by the Society for Endocrinology equipment grant and the North Staffordshire Medical Institute awarded to APS. RAS was funded by Doctoral Alliance/ LJMU funded PhD studentship via APS and further supported by grants awarded to APS from GlaxoSmithKline. PG was funded by EPSRC/MRC (UKRI) PhD studentship via APS and Keele University doctoral training centre and is now supported by the Norwegian School of Sport Sciences. DCH & LMB was supported by the University of Iowa in the laboratory of SCB.

Declarations & Competing Interests

SCB is on the scientific advisory board for Emmyon Inc. The authors declare that they have no other competing interests.

Data Availability Statement

The data that support the findings of this study are available from the corresponding author upon reasonable request.

Acknowledgments

We wish to thank Dr. David S. Waddell (University of North Florida) and Mr. George R. Marcotte (University of Iowa) for technical assistance with the project.

References

1. **Baar K**, **Torgan CE**, **Kraus WE**, **Esser K**. Autocrine Phosphorylation of p70 S6k in Response to Acute Stretch in Myotubes. *Mol Cell Biol Res Commun* 4: 76–80, 2000.
2. **Bentzinger CF**, **Lin S**, **Romanino K**, **Castets P**, **Guridi M**, **Summermatter S**, **Handschin C**, **Tintignac LA**, **Hall MN**, **Rüegg MA**. Differential response of skeletal muscles to mTORC1 signaling during atrophy and hypertrophy. *Skelet Muscle* 3: 1–16, 2013.
3. **Bodine SC**, **Baehr LM**. Skeletal muscle atrophy and the E3 ubiquitin ligases MuRF1 and MAFbx/atrogin-1. *Am J Physiol - Endocrinol Metab* 307: E469–E484, 2014.
4. **Bodine SC**, **Latres E**, **Baumhueter S**, **Lai VKM**, **Nunez L**, **Clarke BA**, **Poueymirou WT**, **Panaro FJ**, **Erqian Na**, **Dharmarajan K**, **Pan ZQ**, **Valenzuela DM**, **Dechiara TM**, **Stitt TN**, **Yancopoulos GD**, **Glass DJ**. Identification of ubiquitin ligases required for skeletal Muscle Atrophy. *Science (80-)* 294: 1704–1708, 2001.
5. **Bodine SC**, **Stitt TN**, **Gonzalez M**, **Kline WO**, **Stover GL**, **Bauerlein R**, **Zlotchenko E**, **Scrimgeour A**, **Lawrence JC**, **Glass DJ**, **Yancopoulos GD**. Akt/mTOR pathway is a crucial regulator of skeletal muscle hypertrophy and can prevent muscle atrophy in vivo. *Nat Cell Biol* 3: 1014–1019, 2001.
6. **Cai C**, **Masumiya H**, **Weisleder N**, **Matsuda N**, **Nishi M**, **Hwang M**, **Ko J**, **Lin P**, **Thornton A**, **Zhao X**, **Pan Z**, **Komazaki S**, **Brotto M**, **Takeshima H**, **Ma J**. MG53 nucleates assembly of cell membrane repair machinery Chuanxi. *Nat Cell Biol* 11: 56–64, 2009.
7. **Cao PR**, **Kim HJ**, **Lecker SH**. Ubiquitin-protein ligases in muscle wasting. *Int J Biochem Cell Biol* 37: 2088–2097, 2005.
8. **Castets P**, **Lin S**, **Rion N**, **Fulvio S Di**, **Romanino K**, **Guridi M**, **Frank S**, **Tintignac LA**, **Sinnreich M**, **Ruegg MA**. Sustained Activation of mTORC1 in Skeletal Muscle Inhibits Constitutive and Starvation-Induced Autophagy and Causes a Severe, Late-Onset Myopathy. *Cell Metab* 17: 731–744, 2013.

9. **Cho JH**, **Kim SA**, **Seo YS**, **Park SG**, **Park BC**, **Kim JH**, **Kim S**. The p90 ribosomal S6 kinase–UBR5 pathway controls Toll-like receptor signaling via miRNA-induced translational inhibition of tumor necrosis factor receptor–associated factor 3. *J Biol Chem* 292: 11804–11814, 2017.

10. **Demonbreun AR**, **McNally EM**. Plasma Membrane Repair in Health and Disease. *Curr Top Membr* 77: 67–96, 2016.

11. **Demonbreun AR**, **Quattrocelli M**, **Barefield DY**, **Allen M V.**, **Swanson KE**, **McNally EM**. An actin-dependent annexin complex mediates plasma membrane repair in muscle. *J Cell Biol* 213: 705–718, 2016.

12. **Drummond MJ**, **Fry CS**, **Glynn EL**, **Dreyer HC**, **Dhanani S**, **Timmerman KL**, **Volpi E**, **Rasmussen BB**. Rapamycin administration in humans blocks the contraction-induced increase in skeletal muscle protein synthesis. *J Physiol* 587: 1535–1546, 2009.

13. **Ebert SM**, **Dyle MC**, **Kunkel SD**, **Bullard SA**, **Bongers KS**, **Fox DK**, **Dierdorff JM**, **Foster ED**, **Adams CM**. Stress-induced skeletal muscle Gadd45a expression reprograms myonuclei and causes muscle atrophy. *J Biol Chem* 287: 27290–27301, 2012.

14. **Eblen ST**, **Kumar NV**, **Shah K**, **Henderson MJ**, **Watts CKW**, **Shokat KM**, **Weber MJ**. Identification of novel ERK2 substrates through use of an engineered kinase and ATP analogs. *J Biol Chem* 278: 14926–14935, 2003.

15. **Goldberg A**. Work-induced growth of skeletal muscle in normal and hypophysectomized rats. *Am J Physiol* 213: 1193–8, 1967.

16. **Gomes MD**, **Lecker SH**, **Jagoe RT**, **Navon A**, **Goldberg AL**. Atrogin-1, A Muscle-Specific F-Box Protein Highly Expressed during Muscle Atrophy Author(s): *PNAS* 98: 14440–14445, 2001.

17. **Goodman CA**, **Frey JW**, **Mabrey DM**, **Jacobs BL**, **Lincoln HC**, **You JS**, **Hornberger TA**. The role of skeletal muscle mTOR in the regulation of mechanical load-induced growth. *J Physiol* 589: 5485–5501, 2011.

18. **Goodman CA**, **Mabrey DM**, **Frey JW**, **Miu MH**, **Schmidt EK**, **Pierre P**, **Hornberger TA**. Novel insights into the regulation of skeletal muscle protein synthesis as revealed by a new nonradioactive in vivo technique . *FASEB J* 25: 1028–1039, 2011.

19. **Hammarström D**, **Øfsteng S**, **Koll L**, **Hanestadhaugen M**, **Hollan I**, **Apró W**, **Whist JE**, **Blomstrand E**, **Rønnestad BR**, **Ellefsen S**. Benefits of higher resistance-training volume are related to ribosome biogenesis. *J Physiol* 598: 543–565, 2020.

20. **Hornberger TA**, **Armstrong DD**, **Koh TJ**, **Burkholder TJ**, **Esser KA**. Intracellular signaling specificity in response to uniaxial vs . multiaxial stretch : implications for mechanotransduction. *Am J Physiol Physiol* 288: C185–C194, 2005.

21. **Hughes DC**, **Baehr LM**, **Discroll JR**, **Lynch SA**, **Waddell DS**, **Bodine SC**. Identification and Characterization of Fbxl22, a novel skeletal muscle atrophy-promoting E3 ubiquitin ligase. *Am. J. Physiol. - Cell Physiol.* (2020). doi: 10.1152/ajpcell.00253.2020.

22. **Hunt LC**, **Stover J**, **Haugen B**, **Shaw TI**, **Li Y**, **Pagala VR**, **Finkelstein D**, **Barton ER**, **Fan Y**, **Labelle M**, **Peng J**, **Demontis F**. A Key Role for the Ubiquitin Ligase UBR4 in Myofiber Hypertrophy in Drosophila and Mice. *Cell Rep* 28: 1268–1281, 2019.

23. **Joseph GA**, **Wang SX**, **Jacobs CE**, **Zhou W**, **Kimble GC**, **Tse HW**, **Eash JK**, **Shavlakadze T**, **Glass DJ**. Partial Inhibition of mTORC1 in Aged Rats Counteracts the Decline in Muscle Mass and Reverses Molecular Signaling Associated with Sarcopenia. *Mol Cell Biol* 39: 1–16, 2019.

24. **Labuzan SA**, **Lynch SA**, **Cooper LM**, **Waddell DS**. Inhibition of protein phosphatase methylesterase 1 dysregulates MAP kinase signaling and attenuates muscle cell differentiation. *Gene* 739: 1–14, 2020.

25. **Macdonald TM**, **Thomas LN**, **Daze E**, **Marignani P**, **Barnes PJ**, **Too CK**. Prolactin-inducible EDD E3 ubiquitin ligase promotes TORC1 signalling , anti-apoptotic protein expression , and drug resistance in breast cancer cells. *Am J Cancer Res* 9: 1484–1503, 2019.

26. **Mcdonald WJ**, **Sangster SM**, **Moffat LD**, **Henderson MJ**, **Too CKL**. a4 Phosphoprotein

494 Interacts With EDD E3 Ubiquitin Ligase and Poly(A)-Binding Protein. *J Cell Biochem* 110:
495 1123–1129, 2010.
496 27. **Miyazaki M**, **Mccarthy JJ**, **Fedele MJ**, **Esser KA**. Early activation of mTORC1 signalling in
497 response to mechanical overload is independent of phosphoinositide 3-kinase/Akt
498 signalling. *J Physiol* 589: 1831–1846, 2011.
499 28. **Moore DR**, **Atherton PJ**, **Rennie MJ**, **Tarnopolsky MA**, **Phillips SM**. Resistance exercise
500 enhances mTOR and MAPK signalling in human muscle over that seen at rest after bolus
501 protein ingestion. *Acta Physiol* 201: 365–372, 2011.
502 29. **Muńoz-Escobar J**, **Matta-Camacho E**, **Kozlov G**, **Gehring K**. The MLLE domain of the
503 ubiquitin ligase UBR5 binds to its catalytic domain to regulate substrate binding. *J Biol Chem*
504 290: 22841–22850, 2015.
505 30. **Nakada S**, **Ogasawara R**, **Kawada S**, **Maekawa T**, **Ishii N**. Correlation between ribosome
506 biogenesis and the magnitude of hypertrophy in overloaded skeletal muscle. *PLoS One* 11:
507 1–14, 2016.
508 31. **Seaborne R.**, **Hughes DC**, **Turner DC**, **Owens DJ**, **Baehr LM**, **Gorski P**, **Semenova EA**, **Borisov**
509 **O V.**, **Larin AK**, **Popov D V.**, **Generozov E V.**, **Sutherland H**, **Ahmetov II**, **Jarvis JC**, **Bodine SC**,
510 **Sharples AP**. UBR5 is a novel E3 ubiquitin ligase involved in skeletal muscle hypertrophy and
511 recovery from atrophy. *J Physiol* 597: 3727–3749, 2019.
512 32. **Seaborne R.**, **Strauss J**, **Cocks M**, **Shepherd S**, **O'Brien T.**, **van Someren K.**, **Bell P.**,
513 **Murgatroyd C**, **Morton J.**, **Stewart C.**, **Mein C.**, **Sharples A.** Data Descriptor : Methylome of
514 human skeletal muscle after acute & chronic resistance exercise training , detraining &
515 retraining. *Sci Data* 5: 1–9, 2018.
516 33. **Seaborne R.**, **Strauss J**, **Cocks M**, **Shepherd S**, **O'Brien T.**, **Van Someren K.**, **Bell P.**,
517 **Murgatroyd C**, **Morton J.**, **Stewart C.**, **Sharples A.** Human Skeletal Muscle Possesses an
518 Epigenetic Memory of Hypertrophy. *Sci Rep* 8: 1–17, 2018.

34. **Seshacharyulu P**, **Pandey P**, **Datta K**, **Batra SK**. Phosphatase : PP2A structural importance , regulation and its aberrant expression in cancer. *Cancer Lett* 335: 9–18, 2013.

35. **Stec MJ**, **Kelly NA**, **Many GM**, **Windham ST**, **Tuggle SC**, **Bamman MM**. Ribosome biogenesis may augment resistance training-induced myofiber hypertrophy and is required for myotube growth in vitro. *Am J Physiol - Endocrinol Metab* 310: E652–E661, 2016.

36. **Wen Y**, **Murach KA**, **Vechetti IJ**, **Fry CS**, **Vickery C**, **Peterson CA**, **McCarthy JJ**, **Campbell KS**. Myo Vision: Software for automated high-content analysis of skeletal muscle immunohistochemistry. *J Appl Physiol* 124: 40–51, 2018.

37. **West DWD**, **Baehr LM**, **Marcotte GR**, **Chason CM**, **Tolento L**, **Gomes A V.**, **Bodine SC**, **Baar K**. Acute resistance exercise activates rapamycin-sensitive and -insensitive mechanisms that control translational activity and capacity in skeletal muscle. *J Physiol* 594: 453–468, 2016.

38. **Williamson D**, **Gallagher P**, **Harber M**, **Hollon C**, **Trappe S**. Mitogen-activated protein kinase (MAPK) pathway activation: Effects of age and acute exercise on human skeletal muscle. *J Physiol* 547: 977–987, 2003.

39. **Xie J**, **Kozlov G**, **Gehring K**. The “tale” of poly(A) binding protein: The MLLE domain and PAM2-containing proteins. *Biochim Biophys Acta - Gene Regul Mech* 1839: 1062–1068, 2014.

40. **Yu M**, **Blomstrand E**, **Chibalin A V.**, **Krook A**, **Zierath JR**. Marathon running increases ERK1/2 and p38 MAP kinase signalling to downstream targets in human skeletal muscle. *J Physiol* 536: 273–282, 2001.